Mathematical Geology, Vol. 38, No. 1, January 2006 (© 2006)
DOI: 10.1007/s11004-005-9001-0

Object Models with Vector Steering[1]

Ragnar Hauge,[2] Anne Randi Syversveen,[2] and Alister MacDonald[3]

Object models are widely used to model the distribution of facies in a reservoir. Several computer programs exist for modelling fluvial channels or more general facies objects. This paper focuses on a marked point model with objects that are able to orient locally according to a vector field. In this way, objects with locally varying curvature are created. With this kind of objects it is possible to model complex depositional basins, that are not easily modelled with conventional methods. The new object type is called Backbone objects. The objects have a piecewise linear centerline and are able to follow the direction of a three-dimensional vector field locally in lateral and vertical direction. How well the objects follow the vector field is determined by three parameters. Use of different coordinate systems and mapping between the systems make it possible to generate Gaussian random fields that follow the shape and direction of the objects. The Gaussian fields can be used to model petrophysical variables, which is important for fluid flow modelling.

KEY WORDS: facies modelling, vector field, Backbone objects, local orientation, turbidites.

INTRODUCTION

Forecasting production of oil and gas is the primary objective of the evaluation of petroleum reservoirs. This involves modelling of fluid flow, which again requires modelling of petrophysical properties such as porosity and permeability. Petrophysical properties often differ from one facies to another, and should be modelled separately for each facies. To do this, a model for the distribution of facies in the reservoir is required. Therefore, a good facies model is of great importance for the petrophysical modelling and indirectly for the fluid flow modelling.

Object models are widely used for facies modelling when the reservoir consists of objects of different facies within a background of some other facies. Modelling of fluvial channels is described by Deutsch and Wang (1996), Holden and others (1998), and Viseur, Shtuka, and Mallet (1998). More general models are

[1]Received 30 July 2003; accepted 11 April 2005; Published online: 20 May 2006.
[2]Norwegian Computing Center, P.O. Box 114, N-0314 Oslo, Norway; e-mail: Anne.Randi.Syversveen@nr.no.
[3]Roxar ASA, Kuala Lumpur, Malaysia.

introduced by Syversveen and Omre (1997) and Lia, Tjelmeland, and Kjellesvik (1996).

The model introduced by Lia, Tjelmeland, and Kjellesvik (1996) has great flexibility in modelling trends in intensity, size, and shape of the objects. The model is also able to condition on complex well observations, but lacks flexibility in local orientation of the objects. It is possible to have trends for rotation and dip of objects, but the trend is a global control of the object, and cannot change direction locally according to the trend. An application of the general model on turbidite reservoirs is described in Yang, Yarus, and Catanese (1999).

The two quite similar papers Jones (1999) and Jones (2001) describe how to locally orient fluvial objects according to a vector field. He generated so called thalwegs, which are centerlines of fluvial deposits conditional to a 2D lateral vector field, and then assigned facies along the centerline. He also described how to construct vector fields from flow paths. In Patterson and others (2002) a similar idea is described, where bar-trains are placed along the thalwegs generated conditional to the vector field.

In this article, we look at an extension of the general marked point model described by Lia, Tjelmeland, and Kjellesvik (1996). To be able to condition to vector fields, we introduce a new type of objects, called the Backbone objects. These objects are able to orient locally according to a vector field in both lateral and vertical directions. Petrophysical variables can be modelled as Gaussian random fields, where the trend and correlation structure follow the local orientation of the objects.

Our approach differs from the thalweg models in that we are able to generate the curved object at once, while Jones (1999) and Patterson and others (2002) first generate the directional paths, and then assign channels or bar-trains to the directional paths. With our approach, we can generate objects of a quite general shape, and we are not restricted to channels or bar-trains. We are also able to condition to vector fields for both lateral and vertical orientation of the objects.

The paper is organized as follows: First, the main ideas of the general marked point model of Lia, Tjelmeland, and Kjellesvik (1996) and Syversveen and Omre (1997) are described. Then we go through the geometry and parametrization of the Backbone objects. Finally, we show how the extended model can be used to model a turbidite reservoir in the Gulf of Mexico, where the orientation of turbidites varies locally, due to local topographical variations. Therefore the Backbone objects are suitable for the modelling.

THE GENERAL MARKED POINT PROCESS

The reservoir is modelled as a marked point model $\mathbf{u} = (\mathbf{u}_1, \mathbf{u}_2, \ldots, \mathbf{u}_n)$, where $\mathbf{u}_i$ is the marked point defining a single facies object. The total number of objects n is stochastic and decided by the intensity distribution, interaction,

and other restrictions included in the model. The marked point process is defined within a rectilinear orthogonal coordinate system called the simulation box, which corresponds to a decompacted reservoir.

The likelihood for a realization **u** given well data **v** and seismic data **s** is given in a Bayesian framework by

$$\pi(\mathbf{u}|\mathbf{v}, \mathbf{s}) \propto \pi_\lambda(\mathbf{u})\pi_I(\mathbf{u})\pi_G(\mathbf{u})\pi_W(\mathbf{v}|\mathbf{u})\pi_S(\mathbf{s}|\mathbf{u}). \tag{1}$$

The different terms control different aspects of the model as follows:

- π_λ: The Poisson point distribution, based on a given intensity field λ, which may be different for different facies. This is a simple point process for each facies.
- π_{I}: A repulsion term between pairs of points. This term and π_λ gives the unconditional point process part of the model. The repulsion may also be facies dependent.
- π_{G}: The distribution of marks. Marks control the size, shape, and orientation of the objects. Together with the two previous terms, this gives an unconditional marked point process.
- π_{W}: The well conditioning term. Since wells are considered as hard data, this term is either 1 (if **u** fits the well data) or 0 (otherwise).
- π_{S}: Term for seismic conditioning. Unlike well data, seismic data are soft, so this is a measure of how good the fit between **u** and the seismic data is.

More details on the different terms can be found in Appendix A.

The idea behind the Bayesian formulation is that it is much simpler to evaluate the likelihood for data given a realization than the other way around. This formulation allows the application of the Metropolis–Hastings algorithm, which in theory can handle arbitrarily complex models. The simplest approach is to draw from the prior distribution and check the data fit, see Deutsch and Wang (1996). However, this can give very slow convergence, so methods that use data to propose reservoirs are preferable, see Lia, Tjelmeland, and Kjellesvik (1996), Syversveen and Omre (1997), and Holden and others (1998).

In this article we propose a new object geometry, which leads to some extension of the term π_G above. All interactions between objects are contained in π_I, so

$$\pi_{\mathrm{G}}(\mathbf{u}) = \prod_i^n \pi_{\mathrm{G}}(\mathbf{u}_i).$$

Furthermore,

$$\mathbf{u}_i = (\mathbf{r}_i, f_i, \theta_i, \Sigma_{\mathrm{i}})$$

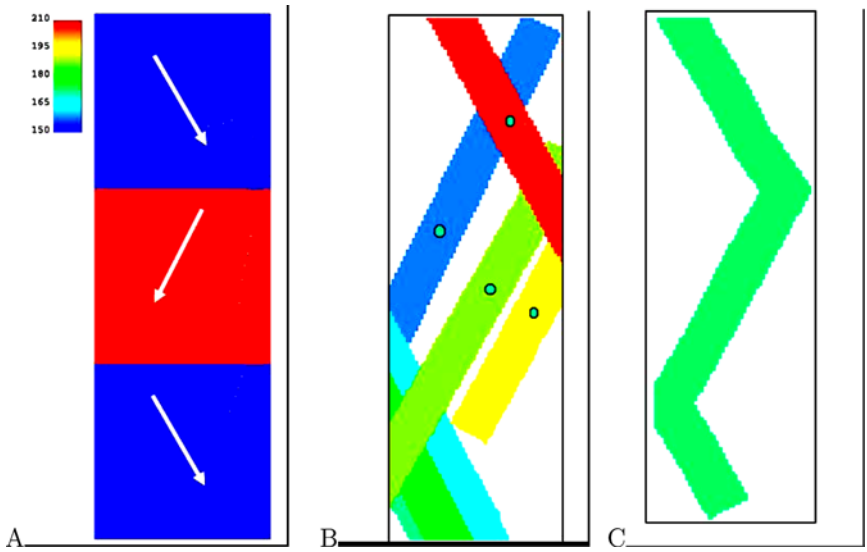

Figure 1. Illustration of the difference between Backbone objects and conventional object shapes. Example of a vector field for rotation, (A), a realization from a conventional object model, (B), and an example of a Backbone object, locally oriented according to the vector field, (C). The dots in B are the objects' reference points.

where $\mathbf{r}_i$ is the location of the object, f_i the facies, θ_i the orientation, and Σ_i the detailed shape. The distributions for θ and Σ may depend on $\mathbf{r}$ and f, but not each other. In the original model, θ consists of two angles, rotation (α) and dip (β), giving each object a global orientation. With the new Backbone objects, these angles become vectors, allowing the object to change direction locally.

BACKBONE OBJECTS

The Backbone objects differ from the objects described above and in Lia, Tjelmeland, and Kjellesvik (1996) in that the orientation varies along the objects, as illustrated in Figure 1. The Backbone objects are able to locally change orientation in space, and follow a vector field. In the following, we describe the parametrization and geometry of the Backbone objects and explain how the objects change direction in space.

Coordinate Systems

As described above, the object model is defined in the simulation box system.

When simulating petrophysical variables for the reservoir, we want the correlation structure to follow the local orientation of the Backbone objects. In addition, we want trends depending on location within the object. To be able to do this, we introduce a local coordinate system for each object. Each object has its own local left-handed orthogonal coordinate system, where the x-axis is along the centerline of the object and positive z direction is downwards. The location of origo is at the center of the object. The objects and the petrophysics are simulated in the local system and mapped to the simbox system. The transformation between coordinate systems is described in Appendix B.

Geometry and Parametrization

As described earlier, each object is characterized by its marks, which are position, shape, size (length, width, thickness), and orientation. The shape of the Backbone objects is specified by a prototype shape in the object's local coordinate system, where the width may vary along the centerline of the object. The width is specified as trend functions symmetrical around the centerline with 1D Gaussian random fields added. Figure 2 shows an example of shape trend in xy plane. The object may also have a thickness profile. As in the original model, Gaussian random fields are added to the top and bottom of the object in the object's local coordinate system in order to condition correctly on well observations. Each object has a reference point which can be located anywhere in the object. The object is placed in the simulation box by drawing the position of the reference point.

The next step is the orientation of the object in the simulation box. For Backbone objects, the parametrization of orientation is complex. The object is divided in pieces of equal length along the centerline, and each of these pieces can have different rotation and dip angle. Each of the pieces will then be able to

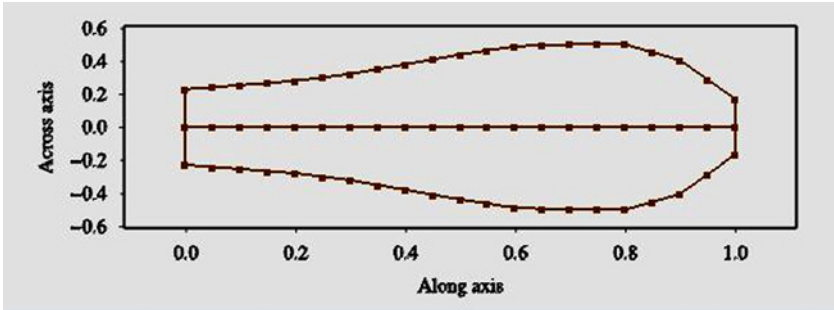

Figure 2. Example of Backbone parametrization in xy plane in local coordinate system. Only trend function is shown.

orient according to the local value of a vector field. The flexible centerline is the object's "backbone."

The connected centerlines of each piece form the centerline of the object ($z = 0$ in the local coordinate system), and angles between pieces are measured as angles between centerline pieces.

Separate 2D vector fields for expected rotation and dip can be defined, together with a corresponding variance, which can be constant or varying in space. Together with the object-specific stiffness parameter defined below, these parameters define the orientation of the Backbone object.

Two parameters specific for the orientation of Backbone objects are given. The first is an approximate piece length, and together with the object length, this defines the number of pieces. The second is a stiffness parameter, that determines the flexibility of the object.

The piece length should be sufficiently short for adapting well to the vector field, and as large as possible for computational reasons.

The stiffness parameter is defined as the standard deviation of the angle between two pieces, and is independent of the variance of rotation and dip. We let α_i be the rotation angle for piece number i, and $\gamma_i = E(\alpha_i)$. The stiffness parameter controls how far the change in direction $\alpha_2 - \alpha_1$ could be from the mean $\gamma_2 - \gamma_1$. The stiffness definition gives the likelihood for α_2, which is Gaussian and given as

$$l_{\mathrm{s}}(\alpha_2) = \text{const} \times \exp(-(\alpha_2 - (\alpha_1 - \gamma_1 + \gamma_2))/\sigma_{\alpha_{\mathrm{s}}})^2, \tag{2}$$

where $\sigma_{\alpha_{\mathrm{s}}}$ is the stiffness parameter. Here we assume a constant stiffness parameter, but generally, the stiffness parameter can be given as a trend function. Similar equations exist for the dip, but in the following we only look at the rotation parameter. We assume that the angle between pieces is Gaussian distributed. The vector field for rotation, together with the rotation variance, defines a Gaussian distribution for the rotation, and the angles for different pieces are independent. The likelihood for α_2 from the vector field is given by

$$l_{\mathrm{v}}(\alpha_2) = \text{const} \times \exp(-(\alpha_2 - \gamma_2)/\sigma_{\alpha_v})^2, \tag{3}$$

where σ_{α_v} is the standard deviation of the vector field, which generally varies in space. Conditional independence of the stiffness and the vector field gives that the conditional distribution for α_2 is Gaussian. By multiplying the two likelihoods given in Equations (2) and (3), we find the conditional mean and variance for α_2 as

$$E(\alpha_2|\alpha_1) = \gamma_2 + \frac{\sigma^2_{\alpha_{\mathrm{v}}}}{\sigma^2_{\alpha_{\mathrm{v}}} + \sigma^2_{\alpha_{\mathrm{s}}}}(\alpha_1 - \gamma_1), \tag{4}$$

and

$$\mathrm{Var}\,(\alpha_2|\alpha_1) = \frac{\sigma^2_{\alpha_v}\sigma^2_{\alpha_s}}{\sigma^2_{\alpha_v} + \sigma^2_{\alpha_s}}. \tag{5}$$

We see that mean is a weighted combination of the means from Equations (2) and (3). For the reference piece of the object, that is, the piece containing the reference point, the variance of the orientation is only decided by the vector field variance.

A proposed object in the Metropolis–Hastings algorithm is drawn as follows: First, draw reference point and size of object. Find the number of pieces based on object length and the approximate piece length. Draw orientation of the reference piece from the distribution defined by the vector field and the corresponding variance. Then draw orientation for the rest of the pieces in both ends conditional to pieces already drawn, starting from the reference piece, using Equations (4) and (5).

Given the reference piece, the stiffness parameter has influence on the orientation of the rest of the pieces. If the stiffness parameter is small and the variance of the vector field is large, the object will not follow the vector field well. But all pieces follow the direction of the reference piece, and objects are smooth in shape. With a large stiffness parameter and large vector field variance, the deviance from the vector field will vary from piece to piece and objects become wiggly. With small vector field variance, the effect of the stiffness parameter is less visible. Figure 3 illustrates this. The objects have a rectangular shape with mean number of pieces equal to 10. The vector field for rotation trend varies from 1° to the left and increases linearly to 60° at the right. Two different constant values are used for the vector field variance and the stiffness parameter. The values are 5 and 25° for both, and the figure shows realizations with the four combinations of these parameter values. The variance is given by Equation (5), and the realizations in Figure 3(B) and (C) have the same variance, however, we see that the realizations are quite different, because the vector field variance and the stiffness parameter are different.

In the thalweg model described by Jones (1999, 2001), the vector field variance is given as a constant, while the stiffness parameter is not present. With this model there is no control of the stiffness of the object except for the vector field variance. This means that objects with a large vector field variance become more wiggly than objects with small vector field variance, and the effect of stiff objects with a large vector field variance shown in Figure 3(C) cannot be reproduced.

MODELLING TURBIDITE RESERVOIRS

Turbidites are deposits from turbidity currents, which are downslope movements of dense, sediment-laden water, see for example Tarbuck and Lutgens

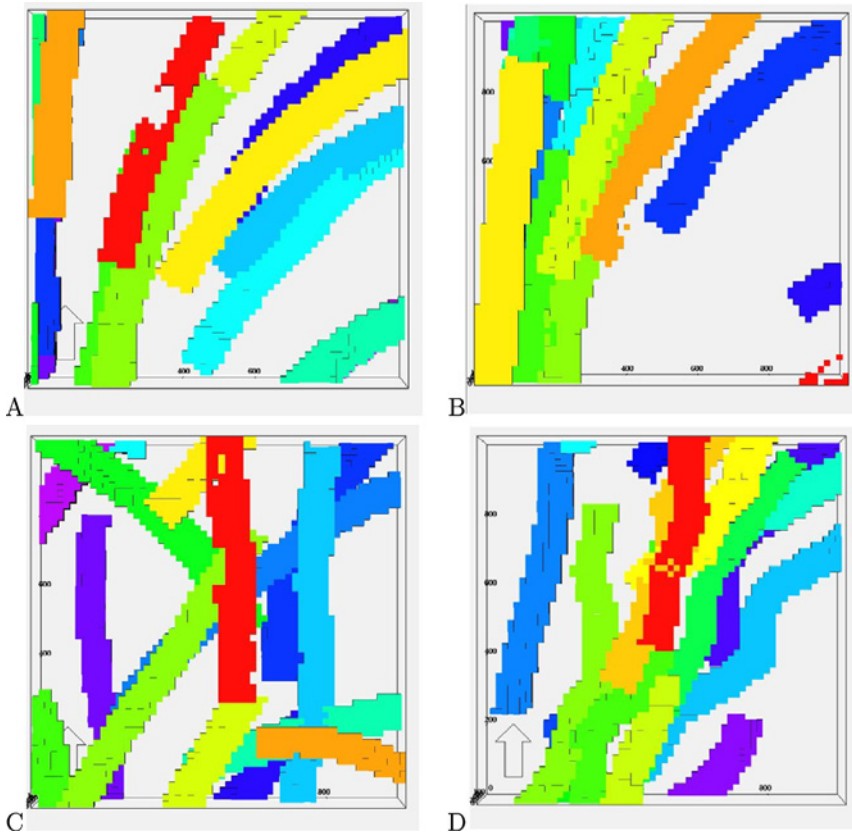

Figure 3. Effect of stiffness parameter and variance of vector field. (A) Small stiffness parameter and small variance. (B) Large stiffness parameter and small variance. (C) Small stiffness parameter and large variance. (D) Large stiffness parameter and large variance.

(1990), p. 485. The local geometry and orientation of the turbidites are therefore strongly controlled by local topographic variations. The local characteristics of the turbidite bodies make the Backbone objects suitable for facies modelling.

Another key feature of turbidity flows is the segregation of grain sizes within flows, which results in systematic spatial trends in petrophysical parameters, (Stow, Reading, and Collinson, 1996). The trends are in three directions—proximal to distal, from axis to margin laterally, and from top to bottom vertically. The use of an object model allows the trends to be preserved in the reservoir model. Petrophysical properties can be simulated separately for each turbidite body using Gaussian random fields in the local coordinate system defined along the backbone.

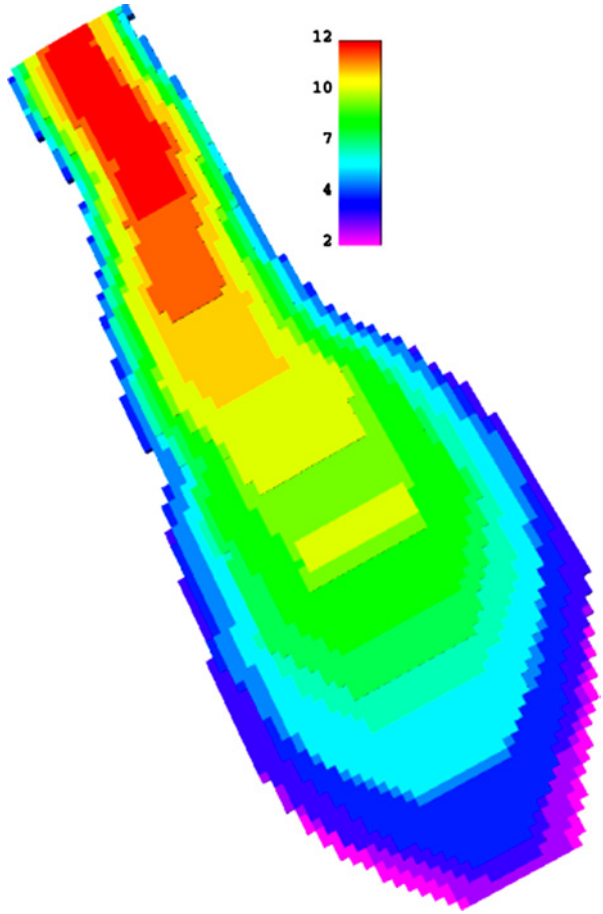

Figure 4. Example of shape of turbidite. The color scale shows thickness of object.

A typical geometry for turbidite reservoirs are lobe-like bodies, which are thick and narrow at the proximal end and become thinner and wider distally. We can construct Backbone objects with such a shape, see Figure 4.

Turbidites have their origin at the same location, and spread out in a fan shape. The location of bodies in an object model is taken care of by the intensity trend. The objects' reference points are placed proportional to the intensity trend. By choosing an intensity trend with very high values in the area we want the objects to start, and small values otherwise, and placing the reference point at the proximal end of the objects, we get the wanted location.

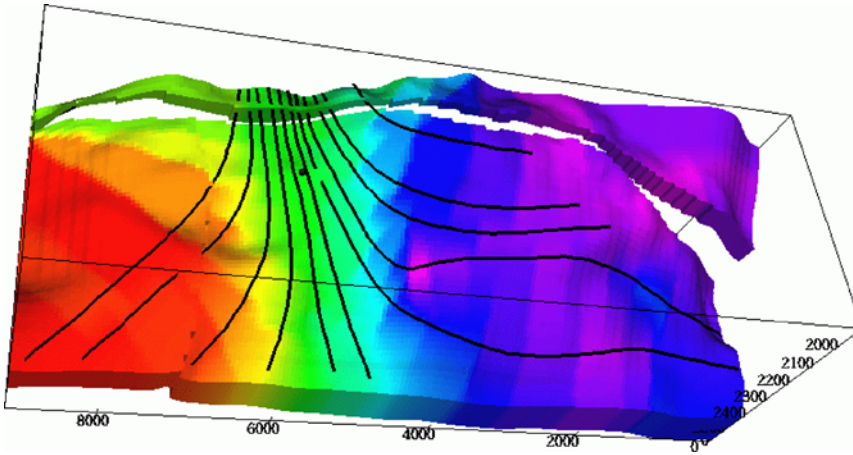

Figure 5. Vector field used for trend of rotation angle.

The fan shape is taken care of by the vector field for rotation trend. The vector field is constructed from flow lines, which can be extracted from the structural interpretation of the reservoir, from isochore information, or directly from seismic data.

Simulation Example

We use the object model with Backbone objects to model a turbidite reservoir in the Gulf of Mexico. A vector field for rotation trend is constructed based on the isochore and geological knowledge, see Figure 5. The flow lines are also shown in the figure. Angles vary between 160 and 320°. The variance of the rotation is held constant equal to 8.0°. There is no trend in dip, and the mean dip is set to zero and the variance is 0.001°. The stiffness parameter is set constant equal to 15.0°. The intensity field has a high value in the area where the flow lines start, see Figure 5, and very small values elsewhere. The shape of the objects is shown in Figure 4. The mean object length is 6000, and mean piece length is 100.

Synthetic well data are generated by simulating an unconditional realization and collecting observations at the well positions. A realization of the turbidite reservoir conditioned to synthetic observations from six wells is shown in Figure 6. The objects start in the high intensity area, and spread out according to the vector field.

Finally, we illustrate how petrophysics can be modelled within each object. Figure 7 shows an example of a porosity realization within a single turbidite object. A Gaussian random field is simulated in the local coordinate system and then transformed to the simbox system. The body is used to create an intrabody

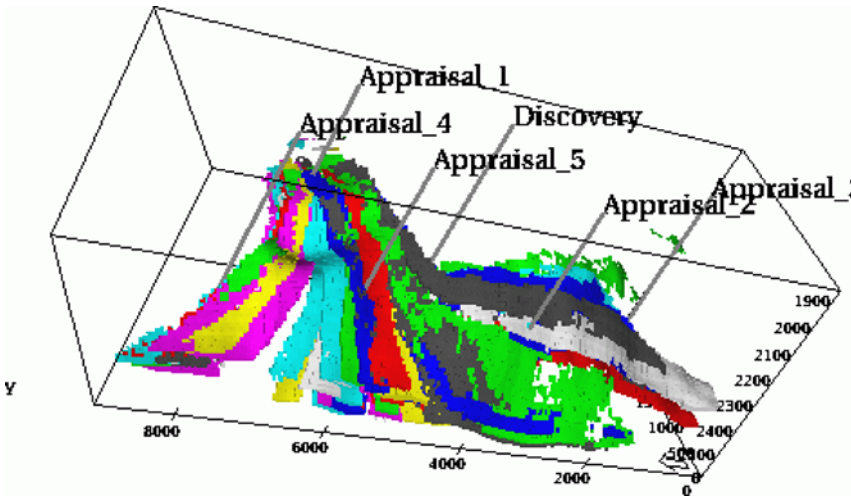

Figure 6. Facies realization for the turbidite reservoir.

trend, where the trend depends on the distance to the edge of the object. We see how the trend follows the shape and orientation of the object. The idea of letting the trend follow the orientation of the object is also described in Jones and Foreman (2003).

A more extensive example of turbidite modelling using Backbone objects is found in Hauge, Syversveen, and MacDonald (2003).

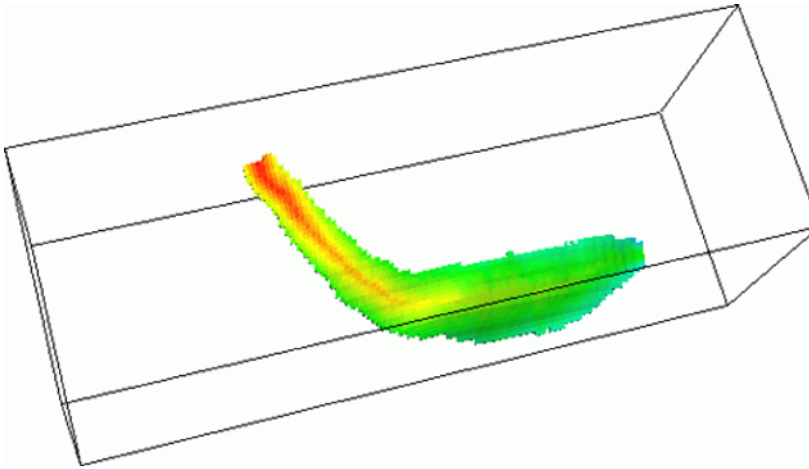

Figure 7. Porosity realization for a single turbidite.

CONCLUDING REMARKS

The Backbone objects provide great flexibility in local orientation of facies objects. Vector fields can be generated from flow paths, and facies objects can be oriented in the direction of the flow paths. Our model is an extension of the marked point model described by Lia, Tjelmeland, and Kjellesvik (1996) that captures the nice features of the thalweg model (Jones, 1999) which allows local orientation of objects according to a vector field. The extended marked point model takes care of the whole facies model with stochastic distributions for location, size, and orientation of objects. The model includes interaction between objects, and multiple well conditioning is taken care of. The thalweg approach, on the other hand, is a method for generating the direction of the objects according to a vector field.

Because of the coordinate systems and the transformation between them, petrophysics is easily generated within each object by using Gaussian random fields.

ACKNOWLEDGMENTS

The authors are grateful to T.E. Jones and another reviewer for valuable comments on an earlier draft of this article.

REFERENCES

Deutsch, C., and Wang, L., 1996, Hierarchial object-based stochastic modeling of fluvial reservoirs: Math. Geol., v. 28, p. 857–880.

Hauge, R., Syversveen, A., and MacDonald, A., 2003, Modeling facies bodies and petrophysical trends in turbidite reservoirs: *in* 2003 Annual Technical Conference and Exhibition: Society of Petroleum Engineers, Denver, CO, SPE paper no. 84053, 7 p on CD.

Holden, L., Hauge, R., Skare, O., and Skorstad, A., 1998, Modelling of fluvial reservoirs with object models: Math. Geol., v. 30, no. 5, p. 473–496.

Jones, T., 1999, Controlling body orientation in object-based modeling: Flowpaths and vector fields, *in* Lippard, S. Næss, A., and Sinding-Larsen, R., eds., Proceedings of the 5th annual conference of the International Association for Mathematical Geology, v. 2: Tapir, Tronhdeim, Norway, p. 633–638.

Jones, T., 2001, Using flowpaths and vector fields in object-based modeling: Comput. & Geosci., v. 27, p. 133–138.

Jones, T., and Foreman, J., 2003, Azimmod: Method to honor channel directionality when building 3-d petrophysical models: Comput. & Geosci., v. 29, p. 1033–1044.

Lia, O., Tjelmeland, H., and Kjellesvik, L., 1996, Modelling of facies architecture by marked point models: *in* Baafi, E., and Schofield, N., eds., Geostatistics Wollongong '96, v. 1: Kluwer Academic, Dordrecht, The Netherlands, p. 386–397.

Patterson, P., Jones, T., Donofrio, C., Donovan, A., and Ottmann, J., 2002, Geologic modelling of external and internal reservoir architecture of fluvial depositional systems: *in* Armstrong, M.,

Bettini, C., Champigny, N., Galli, A., and Remacre, A., eds., Geostatistics Rio 2000: Kluwer Academic, Dordrecht, The Netherlands, p. 41–52.

Stow, D., Reading, H., and Collinson, J., 1996, Deep seas: *in* Reading, H., ed., Sedimentary environments, processes, facies and stratigraphy: Blackwell Sciences, Oxford, p. 395–453.

Syversveen, A. R., and Omre, H., 1997, Conditioning of marked point processes within a Bayesian framework: Scand. J. Stat., v. 24, no. 3, p. 341–352.

Tarbuck, E., and Lutgens, F., 1990, The Earth: Macmillian, New York, 651 p.

Viseur, S., Shtuka, A., and Mallet, J., 1998, New fast, stochastic, boolean simulation of fluvial deposits: *in* 1998 Annual Technical Conference and Exhibition: Society of Petroleum Engineers, New Orleans, LA, SPE paper no. 49281, p. 697–709.

Yang, K., Yarus, J., and Catanese, W., 1999, Characterization and 3-D modeling of turbidite reservoir: A case study in miocene slope deposits, Main Pass Area, offshore Gulf Coast of Mexico: *in* Gulf Coast Association of Geological Societies Transactions, v. XLVIIII, p. 54–61.

APPENDIX A

The different terms in the marked point model (Equation (1)) are explained in more detail here. The Poisson point distribution is given by

$$\pi_\lambda(\mathbf{u}) = \frac{1}{n!}\prod_{i=1}^{n}\lambda(f_i, \mathbf{r}_\mathrm{i}),$$

that is, the intensity depends on location and facies.

The repulsion term is given by

$$\pi_\mathrm{I}(\mathbf{u}) = \exp\left(-\sum_{i=1}^{n}\sum_{j=i+1}^{n} b(f_i, f_j, \mathbf{r}_\mathrm{i} - \mathbf{r}_\mathrm{j})\right),$$

where b is the pairwise repulsion function. It depends only on the facies and the relative distance between two objects, so the order of i and j is irrelevant. The distance is typically weighted so that distance along the z-axis is magnified, since this typically is a much shorter scale in a reservoir. The repulsion falls to zero as the distance increases. A typical example is the Strauss process, where the repulsion is constant for all distances below a threshold, and zero otherwise.

The most complicated term is the geometric term. As stated before,

$$\mathbf{u}_\mathrm{i} = (\mathbf{r}_\mathrm{i}, f_i, \theta_i, \Sigma_\mathrm{i}),$$

and the geometric term can be written

$$\pi_\mathrm{G}(\mathbf{u}_\mathrm{i}) = \pi_\mathrm{G}(\theta_i, \Sigma_\mathrm{i}|\mathbf{r}_\mathrm{i}, f_i)\ .$$

This means that all geometric parameters depend on facies and location. The detailed shape Σ is given by

$$\Sigma = (T, l, w, h, R^L, R^R, R^T, R^B),$$

where T is the basic shape of the object; l, w and h are the length, width, and height of the object; and R^{L}, R^{R}, R^{T} and R^{B} are Gaussian fields modifying the right and left edge, and top and bottom of the object. The basic shape T is given as a two-dimensional shape with two axes, length and width, see Figure 2. Two thickness trends, one along and one across the object define the thickness shape. For l,w, and h, a multi-Gaussian distribution is used, truncated so that only positive values are allowed.

Since the well term is a simple binary, no further explanation of that is needed. The seismic term is given by

$$\pi_{\mathrm{S}}(\mathbf{u}) = \prod_k g(s_k | f_k)^a,$$

where the product now is over grid cells in a gridded realization, f_k is the facies in cell k, and s_k is the value of the seismic parameter there. The function $g(s|f)$ is the likelihood for seismic value s given facies f, and a is a scaling factor. The function g is defined from well logs and seismic data. The expression would be correct with $a = 1$ if all cells had independent values. Since this is not the case, a is set somewhere between zero and one, depending on the correlations involved.

APPENDIX B

During simulation, we sometimes operate in the object's local coordinate system, and sometimes in the global simulation box system. The parametrization of the object is simpler in the local system, particularly for the Gaussian fields for top, bottom, and edges. Well conditioning is therefore done in the local system. Each piece of the object has its own orientation, hence the transformation between the coordinate systems is very complex.

When transforming a point from the simulation box system to the local coordinate system, we do as follows:

- Find which piece the point belongs to, as described later.
- Do a rotation and translation, such that origo is in the center of the centerline of the actual piece, and rotation and dip angles are zero.
- Transform to a nonorthogonal coordinate system, called NonOrto. See Figures 8 and 9.
- Transform to the local coordinate system by "stretching" out the object.

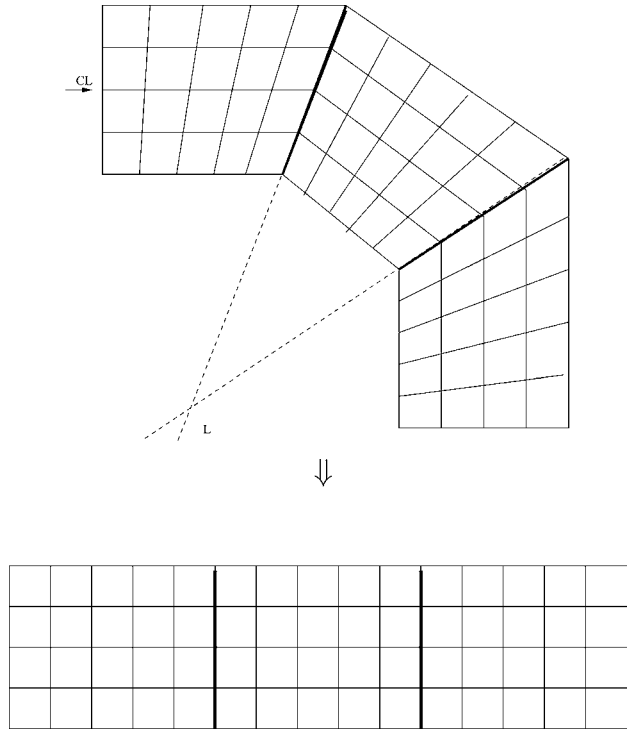

Figure 8. Object in NonOrto and local coordinate system. *Thick lines* are borders between pieces, *thin lines* are borders between grid cells. CL is the centerline, also called the "backbone" of the object.

The NonOrto system is a nonorthogonal system for a single piece, constructed as follows: First define end planes, which are border planes between pieces. These are the set of points with equal distance to the midpoint of the centerlines on each side. The centerline is marked with *CL* in Figure 8. At the ends of the object, this plane is orthogonal to the centre line. The end planes for the middle piece are marked with dotted lines in Figure 8. The intersection of the end planes defines a line called *L* in the figure. (Since the figure is two-dimensional, it is a point in the figure.) The lines across the object represent constant x-values. The x-coordinate of a point is defined by the intersection between *CL* and the plane given by the point and the line *L*. Origo is placed in the middle of the piece.

A point is defined if it is located inside the "fan" defined by the end planes. If the point is in multiple fans, its x-coordinate is given from the centerline closest to the point. Objects with undefined points will be rejected during simulation.

In each piece, the y- and z-coordinates are measured along axes that are orthogonal to each other and the local centerline. Ideally, we would like the

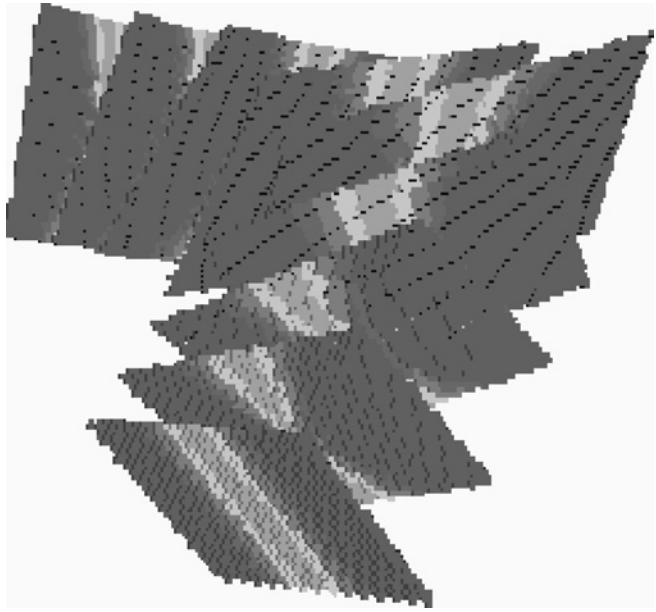

Figure 9. Illustration of rotation of coordinate systems. The figure shows cross sections of an object in the simulation box. Each section is at a constant local x-coordinate, and the lines are parallel to the local z-axis for the object.

z-axis to be in the plane defined by this centerline and the z-axis of the simulation box. This would give the most logical interpretation of object thickness, top and bottom. However, this would lead to inconsistency in the end planes, since the z-axis from two neighboring pieces would not correspond if either the dip or the rotation are different for the two pieces. To avoid this, the y-z plane is rotating around the x-axis. In the middle of the piece, the z-axis has our ideal orientation, whereas it is rotated toward the end planes in such a way that the z-axes from neighboring pieces match in the end planes, and have the same rotation from the center of the piece. The y-axis follows this rotation, so that it is always orthogonal to the z-axis and the centerline; see Figure 9 for an illustration. The figure shows how cross sections with constant x in the local system are oriented in the simulation box, as well as the direction of the local z-axis.

The last step from NonOrto to the local system is to adjust the x-coordinate such that zero is in the middle of the object, and not in the middle of the selected piece. Note that this final coordinate system is treated as orthogonal when needed, it is only nonorthogonal seen from the simulation box.

All steps are easily reversed, and we go from the local system to the simulation box by doing all the steps in the opposite order.